AIP | Applied Physics Letters

Inkjet printed silver nanowire network as top electrode for semi-transparent organic photovoltaic devices

Hui Lu, Jian Lin, Na Wu, Shuhong Nie, Qun Luo, Chang-Qi Ma, and Zheng Cui

Citation: Applied Physics Letters **106**, 093302 (2015); doi: 10.1063/1.4913697
View online: http://dx.doi.org/10.1063/1.4913697
View Table of Contents: http://scitation.aip.org/content/aip/journal/apl/106/9?ver=pdfcov
Published by the AIP Publishing

Articles you may be interested in

Dense nanoimprinted silicon nanowire arrays with passivated axial p-i-n junctions for photovoltaic applications
J. Appl. Phys. **117**, 125104 (2015); 10.1063/1.4916535

Ag nanowire percolating network embedded in indium tin oxide nanoparticles for printable transparent conducting electrodes
Appl. Phys. Lett. **104**, 071906 (2014); 10.1063/1.4866007

Performance improvement of inverted polymer solar cells by doping Au nanoparticles into TiO2 cathode buffer layer
Appl. Phys. Lett. **103**, 233303 (2013); 10.1063/1.4840319

Transparent metal electrodes from ordered nanosphere arrays
J. Appl. Phys. **114**, 054502 (2013); 10.1063/1.4816790

Non-contact printing of high aspect ratio Ag electrodes for polycrystalline silicone solar cell with electrohydrodynamic jet printing
Appl. Phys. Lett. **102**, 123901 (2013); 10.1063/1.4798332

Reuse of AIP Publishing content is subject to the terms at: https://publishing.aip.org/authors/rights-and-permissions. Download to IP: 141.215.185.157 On: Mon, 19 Sep 2016 13:23:39

Inkjet printed silver nanowire network as top electrode for semi-transparent organic photovoltaic devices

Hui Lu, Jian Lin,[a] Na Wu, Shuhong Nie, Qun Luo, Chang-Qi Ma,[b] and Zheng Cui
Printable Electronics Research Centre, Suzhou Institute of Nano-Tech and Nano-Bionics, Chinese Academy of Sciences, No. 398 Ruoshui Road, SEID, Suzhou Industrial Park, Suzhou, Jiangsu 215123, People's Republic of China

(Received 21 January 2015; accepted 16 February 2015; published online 5 March 2015)

A method for direct inkjet printing of silver nanowire (Ag NW) to form transparent conductive network as the top electrode for inverted semi-transparent organic photovoltaic devices (OPV) was developed. The highest power conversion efficiency of the poly(3-hexylthiophene):phenyl-C61–butyric acid methyl ester (P3HT:$PC_{61}BM$) based OPV was achieved to be 2.71% when the top electrode was formed by 7 times of printing. In general, devices with printed Ag NW top electrode had similar open-circuit voltage (V_{OC}, around 0.60 V) but lower fill factor (*FF*, 0.33–0.54) than that of device with thermally deposited Ag opaque electrode (reference device). Both *FF* and short-circuit current density (J_{SC}), however, were found to be increasing with the increase of printing times (3, 5, and 7), which could be partially attributed to the improved conductivity of Ag NW network electrodes. The solvent effect on device performances was studied carefully by comparing the current density-voltage (*J-V*) curves of different devices. The results revealed that solvent treatment on the anode buffer layer during printing led to a decrease of charge injection selectivity and an increase of charge recombination at the anode interface, which was considered to be the reason for the degrading of device performance. © *2015 AIP Publishing LLC*.
[http://dx.doi.org/10.1063/1.4913697]

Transparent electrode is one of the critical components for transparent optoelectronic devices, especially in semi-transparent solar cells[1–3] for building integrated photovoltaic applications. Several types of transparent conductors, including conductive polymers,[4] carbon nanotubes,[5] graphenes,[6] and metal meshes[7,8] have been extensively investigated for use as flexible and low-cost electrodes to replace traditional indium tin oxide (ITO) electrode. Among them, solution-processed silver nanowire (Ag NW) networks show excellent transparency, electrical conductivity, and mechanical flexibility and have received substantial attentions in the last few years.[9] With respect to Ag NW electrode for organic photovoltaics (OPV), most of Ag NW networks were used as bottom electrode and organic layers were deposited on top of it.[10–13] Only a few papers reported Ag NW as top electrode in OPV through lamination,[14] spray,[15] or drop-casting[16] approaches, none of which were direct patterning. Although inkjet printing is one of the most feasible approaches for top electrode deposition, inkjet printing of AgNW as top electrode for organic solar cells has not been reported yet. The reason may arise from the challenge of nozzle clogging in inkjet printing.

For organic solar cells, solution-processed poly(3,4-ethylenedioxythiophene):poly(styrenesulfonate) (PEDOT:PSS) is the most well-known anode buffer layer owing to its suitable work function (WF), good charge transport ability, and excellent visible light transparency.[17] However, solvents contained in Ag NW inks may incur damage to the underlying PEDOT:PSS layer. In addition, physical and chemical interactions between the conductive ink and the organic layer may affect the wettability which would lead to poor quality of film formation during inkjet printing. In this letter, inkjet printing of Ag NW networks as top electrode for inverted semi-transparent organic solar cells was reported. The performance of these solar cells was tested and compared to those having conventional top electrodes. The influence of ink solvents on charge injection properties at the interface between photoactive layer and Ag NW top electrode was characterised to evaluate the "printing effect" on the device performance.

Ag NW purchased from Blue Nano was dispersed in the mixture of 75% ethanol and 25% ethylene glycol (EG) to form a 0.35 mg/ml suspension. The formulated Ag NW ink was printed by MicroFab jetlab II inkjet printer in multi-pass (3, 5, 7, and 9 times) on the surface of spin-coated PEDOT:PSS:MoO_3 layer on a glass substrate. The nozzle clogging during inkjet printing was eliminated by adding high boiling point EG into the Ag NW ink to reduce the ink evaporation in the print head.[18] Fig. 1(a) shows the optical transmittance and sheet resistance of inkjet printed Ag NW networks. It is obvious that the sheet resistance of printed Ag NW decreases dramatically from 2190 Ω/□ to 26.4 Ω/□ with the increase of printing times from 3 to 9, whereas the average transparency of the printed Ag NW over 400–800 nm wavelength decreases slightly from 95% to 83%. Note that the 7 times printed Ag NW layer has an average sheet resistance of 44.9 Ω/□ and an average transparency of 86.4%, which are close to that of widely used ITO electrode. Fig. 1(b) shows the Scanning Electron Microscope (SEM) images of printed Ag NW. As can be seen here, the distribution of inkjet printed Ag NW is not uniform and Ag NW aggregate on the PEDOT:PSS:MoO_3 surface. Note that no surface treatment was performed prior to Ag NW printing, therefore, the

[a]jlin2010@sinano.ac.cn
[b]cqma2011@sinano.ac.cn

 © 2015 AIP Publishing LLC

Reuse of AIP Publishing content is subject to the terms at: https://publishing.aip.org/authors/rights-and-permissions. Download to IP: 141.215.185.157 On: Mon, 19 Sep 2016 13:23:39

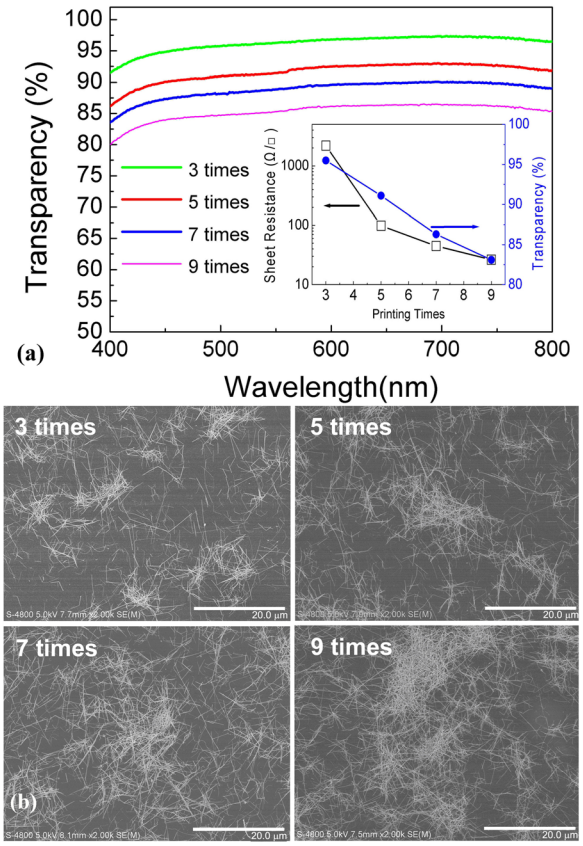

FIG. 1. The transparency (a) and SEM images (b) of the inkjet printed Ag NW on PEDOT:PSS:MoO_3/Glass surface. The inset in figure (a) shows the average sheet resistances and transmissions of the Ag NW networks of different printing times.

aggregation of Ag NW could be due to the poor wettability between the Ag NW ink and the anode buffer layer. This could be the reason that the printed Ag NW electrode showed higher sheet resistance than that of spin coated Ag NW networks.[19] Though there are many methods to modify surface energy, to make the top surface of organic layer into hydrophilic without electrical performance degradation is still a challenge.

The layer structure of inverted organic solar cells is shown in Fig. 2(a), which consists of ITO/ZnO (25 nm)/P3HT:$PC_{61}BM$ (1:1 w/w, 175–185 nm)/PEDOT:PSS:MoO_3 (40–50 nm)/Ag NW. P3HT:$PC_{61}BM$ is the photoactive layer[20] and the specially formulated PEDOT:PSS:MoO_3 is used as the anode buffer layer to improve film quality.[21] Only the Ag NW electrode layer was inkjet-printed, while all the other layers were deposited by spin-coating. The Ag NW was printed in ambient in multi pass printing of 3, 5, 7, and 9 times and the corresponding solar cells were marked as devices A_{3T}, A_{5T}, A_{7T}, and A_{9T}, respectively. No additional surface treatment was performed on the PEDOT:PSS:MoO_3 layer prior to printing Ag NW. For comparison, two types of reference solar cells were made and tested: one with printed PEDOT:PSS:MoO_3 layer and thermally evaporated Ag top electrode (marked as device B); another having printed solvent onto the PEDOT:PSS:MoO_3 layer before evaporating the Ag electrode (marked as device C). Current density versus voltage (*J-V*) curves were measured with a Keithley 2400 source meter in nitrogen ambient under dark and under simulated solar light (~100 mW/cm^2) generated by white light from a halogen tungsten lamp, filtered by a Schott GG385 UV filter and a Hoya LB120 daylight filter.[22] The UV-Vis-NIR absorption spectra of the polymer films were taken with a Lambda 750 UV/VIS Spectrometer. The thicknesses of each layer were determined with an Alpha 500 step profiler. A Hitachi S-4800 Field Emission SEM was used to inspect the printed Ag NW film.

Fig. 2(b) depicts the UV-Vis absorption spectra of the solar cells with Ag NW electrode. Although the absorbance

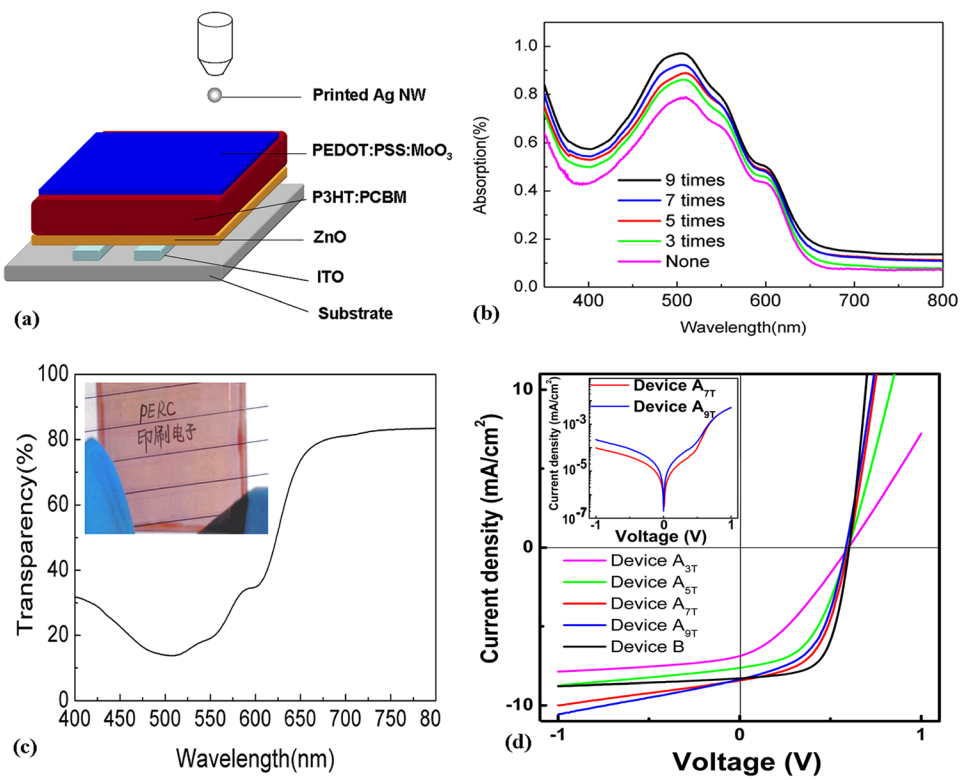

FIG. 2. (a) The schematic structure of the inverted device with printed Ag NW electrodes, (b) the absorption of device before and after printing Ag NW, (c) the transparency of device A_{7T} with the picture in the inset, and (d) typical *J-V* characteristics of the OPV devices with inkjet printed Ag NW top electrode and thermal deposited Ag top electrode. The inset in figure (d) shows the comparison of dark *J-V* curves between devices A_{7T} and A_{9T}.

Reuse of AIP Publishing content is subject to the terms at: https://publishing.aip.org/authors/rights-and-permissions. Download to IP: 141.215.185.157 On: Mon, 19 Sep 2016 13:23:39

of complete device increased gradually with the increase of printing times, due to the decrease of transparency of Ag NW electrode (Fig. 1(a)), all these devices showed typical absorption features of P3HT:$PC_{61}BM$ layer,[23] suggesting no spectral alteration caused by the top Ag NW electrode on the photoactive layer. All these devices showed the highest absorption of 86% peaked at 500 nm. Because of the transparent Ag NW top electrode, these solar cells are generally semi-transparent, as the inset picture shown in Fig. 2(c), with an average transparency of 57% over the entire visible wavelength (400–800 nm). Photovoltaic properties of solar cells with inkjet printed Ag NW top electrode (device A) were measured and the characteristics were compared with that of the reference device B, which had thermally deposited opaque Ag layer as the top electrode. Fig. 2(d) shows the *J-V* curves of these devices and all the PV performance data are listed in Table I. Both J_{SC} and *FF* increased significantly from devices A_{3T} to A_{7T} with the same V_{OC}. This could be partially attributed to the decrease of sheet resistance (Fig. 1(a)). However, the device performance started to deteriorate when the Ag NW was printed for more than 7 times. The decrease of performance for device A_{9T} was mainly due to the decrease of V_{OC} and *FF* (Table I). A comparison on the dark *J-V* curves of the devices A_{9T} and A_{7T} (Figure 2(d), inset) clearly showed that device A_{9T} had higher dark reverse current *J* than device A_{7T}, although both devices had similar current density *J* at 0.7–1.0 V. Such a higher leakage current at reversed bias suggested that poorer electron blocking ability of the MoO_3:PEDOT:PSS layer after printing with Ag for 9 times, which was ascribed to the undesirable solvent effect. As a result, the best power conversion efficiency (PCE) was 2.71% (device A_{7T}), which was slightly lower than the PCE of reference device B (3.15%). Detailed comparisons showed that device A_{7T} has slightly higher J_{SC} but lower *FF* compared to device B, whereas all these devices had the same V_{OC} of 0.60 V. Considering the device structure, the possible reason of device performance decrease could be due to the change of charge injection layer (PEDOT:PSS:MoO_3) rather than the change of active (P3HT:PCBM) layer during the printing process.[24,25]

To better understand the influence of ink solvent on device performance during printing, two different solar cells having the same thermal deposited Ag electrode were fabricated and tested (devices B and C). The only difference between these two cells was that the PEDOT:PSS:MoO_3 layer of device C was covered with solvent before thermal deposition of Ag electrode. It is interesting to notice from Table I that device C had almost identical device performance to device A_{7T}. The comparison of Figs. 2(d) and 3(a) confirms the similarity. In Fig. 3(b), the dark current of device C at inverses bias was much higher than device B, while they had similar current density *J* at 0.6–1.0 V. So the rectification ratio of device B at ±1 V was 1698, while that of device C was only 32.9.

TABLE I. Device performances of the OPV devices with different top electrodes of which the *J-V* characteristics are shown in Figs. 2 and 3.

Device	Jsc (mA·cm^2)	Voc (V)	*FF*	PCE (%)
A_{3T}	6.88	0.60	0.33	1.36
A_{5T}	7.63	0.60	0.49	2.24
A_{7T}	8.44	0.60	0.54	2.71
A_{9T}	8.37	0.58	0.52	2.51
B	8.30	0.60	0.63	3.15
C	8.28	0.60	0.54	2.67

To elucidate the current transport mechanism leading to such a big difference, the dark currents of devices B and C at negative voltage were studied. The *J-V* characteristic of device B at negative voltage in Fig. 3(c) showed quite good straight line in plot of ln *J* vs $V^{1/2}$ at −0.3−−1.0 V. This straight line relation indicates that the conduction mechanism is Richardson-Schottky (RS) thermionic emission,[26] which is a kind of injection limited current. On the other hand, the *J-V* curve of device C at −0.01−−1.0 V in Fig. 3(d) had a slope of 0.9–1.2 in plot of log *J* vs log *V*, which is a typical phenomenon of Ohmic conduction with low injection barrier. The comparison of dark currents at negative voltage showed that device C should have a much lower electron injection barrier than device B at the interface of anode (PEDOT:PSS:MoO_3/Ag), which led to a much higher dark current.

To interpret the mechanism of lower *FF* and smaller R_{sh} in devices A and C, their schematic energy band diagrams of are depicted in Fig. 4. As discussed above, the PEDOT:PSS:MoO_3 layers were proved to have lower electron injection barrier after the solvent treatment (Fig. 4(b)), which means that the metal/organic contact has lower selectivity for the extraction of two types of charge carriers than the device without solvent treatment (shown in Fig. 4(a)). As a result, there were more recombination between holes and electrons at the solvent treated interface of anode (P3HT:PCBM/PEDOT:PSS:MoO_3/Ag), which were attributed to the lower *FF* and smaller R_{sh}.[27,28] On the other hand, the V_{OC} of most devices was kept at 0.6 V except device A_{9T}, suggesting that the hole can still inject with the same barrier, and

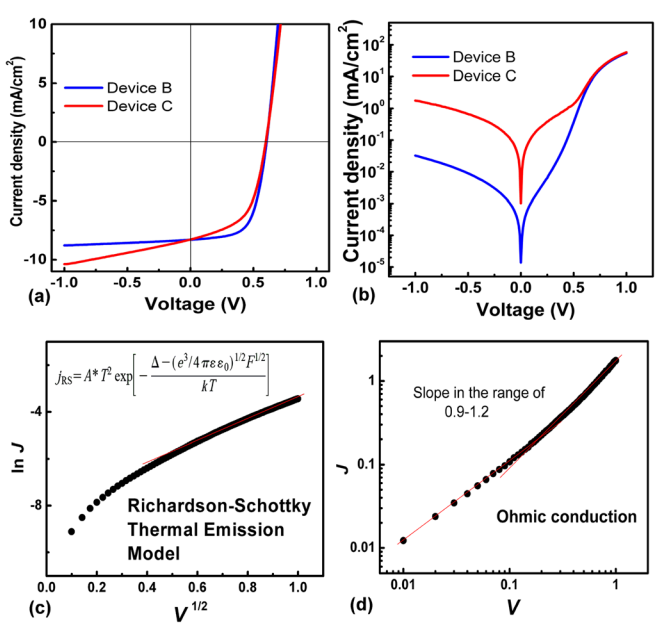

FIG. 3. Top: Comparisons of typical light (a) and dark (b) *J-V* curves between devices B and C. Bottom: Dark *J-V* curve analysis of devices B (c) and C (d).

Reuse of AIP Publishing content is subject to the terms at: https://publishing.aip.org/authors/rights-and-permissions. Download to IP: 141.215.185.157 On: Mon, 19 Sep 2016 13:23:39

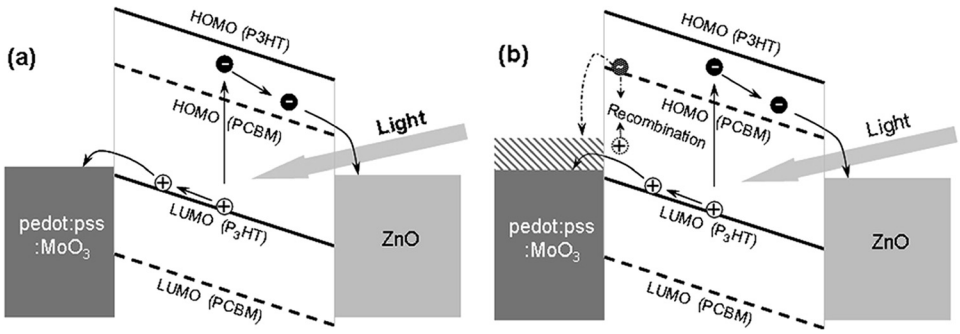

FIG. 4. Schematic band diagrams of the device B (a) and device A/C (b).

was finally increased after the solvent printed for 9 times.[29] The poorer electron blocking of the 9 times printed MoO_3:PEDOT:PSS layer leading to the lower *FF* than device A_{7T}, though the printed electrode has lowest resistance.

In summary, we have demonstrated a direct inkjet printed transparent Ag NW network as the top electrode for OPV device. With the increase of printing times, the conductivity of Ag NW increases dramatically, while the transparency of the electrode decreases only slightly. The best power conversion efficiency of 2.71% was achieved for P3HT: $PC_{61}BM$ based device having 7-times printed Ag NW top electrode. The achieved efficiency is slightly lower than that of thermally evaporated Ag electrode (3.15%). Solvent effect on the top of anode buffer layer during printing of Ag NW was found to be the main reason for the decrease of device performance, which originated from the decrease of charge carrier injection selectivity, leading to an increased charge recombination rate at the anode buffer layer/Ag NW interface. The direct inkjet printing of Ag NW top electrode and the related solvent effect studies open up the possibility of making semi-transparent solar cells and associated applications.

This work was supported by the project of the Major Research plan of the National Natural Science Foundation of China (Grant No. 91123034), National Natural Foundation of China (Grant No. 21003153), Strategic Priority Research Program of the Chinese Academy of Sciences (Grant No. XDA09020201), and Project supported by National Science and Technology Ministry (Grant No. 2012BAF13B05-402).

[1]R. R. Lunt, Appl. Phys. Lett. **101**, 043902 (2012).
[2]Y. Zhao and R. R. Lunt, Adv. Energy Mater. **3**, 1143 (2013).
[3]R. Betancur, P. Romero-Gomez, A. Martinez-Otero, X. Elias, M. Maymo, and J. Martorell, Nat. Photonics **7**, 995 (2013).
[4]Y. H. Ha, N. Nikolov, S. K. Pollack, J. Mastrangelo, B. D. Martin, and R. Shashidhar, Adv. Funct. Mater. **14**, 615 (2004).
[5]Z. C. Wu, Z. H. Chen, X. Du, J. M. Logan, J. Sippel, M. Nikolou, K. Kamaras, J. R. Reynolds, D. B. Tanner, A. F. Hebard, and A. G. Rinzler, Science **305**, 1273 (2004).
[6]X. Wang, L. J. Zhi, and K. Mullen, Nano Lett. **8**, 323 (2008).
[7]J. Y. Lee, S. T. Connor, Y. Cui, and P. Peumans, Nano Lett. **8**, 689 (2008).
[8]J. Y. Zou, H. L. Yip, S. K. Hau, and A. K. Y. Jen, Appl. Phys. Lett. **96**, 203301 (2010).
[9]D. Langley, G. Giusti, C. Mayousse, C. Celle, D. Bellet, and J. P. Simonato, Nanotechnology **24**, 452001 (2013).
[10]C. Sachse, L. Muller-Meskamp, L. Bormann, Y. H. Kim, F. Lehnert, A. Philipp, B. Beyer, and K. Leo, Org. Electron. **14**, 143 (2013).
[11]D. Angmo and F. C. Krebs, J. Appl. Polym. Sci. **129**, 1 (2013).
[12]W. Gaynor, G. F. Burkhard, M. D. McGehee, and P. Peumans, Adv. Mater. **23**, 2905 (2011).
[13]M. Song, D. S. You, K. Lim, S. Park, S. Jung, C. S. Kim, D. H. Kim, D. G. Kim, J. K. Kim, J. Park, Y. C. Kang, J. Heo, S. H. Jin, J. H. Park, and J. W. Kang, Adv. Funct. Mater. **23**, 4177 (2013).
[14]J. Y. Lee, S. T. Connor, Y. Cui, and P. Peumans, Nano Lett. **10**, 1276 (2010).
[15]J. Krantz, T. Stubhan, M. Richter, S. Spallek, I. Litzov, G. J. Matt, E. Spiecker, and C. J. Brabec, Adv. Funct. Mater. **23**, 1711 (2013).
[16]M. Reinhard, R. Eckstein, A. Slobodskyy, U. Lemmer, and A. Colsmann, Org. Electron. **14**, 273 (2013).
[17]R. Po, C. Carbonera, A. Bernardi, and N. Camaioni, Energy Environ. Sci. **4**, 285 (2011).
[18]A. Lange, M. Wegener, C. Boeffel, B. Fischer, A. Wedel, and D. Neher, Sol. Energy Mater. Sol. Cells **94**, 1816 (2010).
[19]D. S. Leem, A. Edwards, M. Faist, J. Nelson, D. D. C. Bradley, and J. C. de Mello, Adv. Mater. **23**, 4371 (2011).
[20]M. T. Dang, L. Hirsch, and G. Wantz, Adv. Mater. **23**, 3597 (2011).
[21]Y. Wang, Q. Luo, N. Wu, Q. Wang, H. Zhu, L. Chen, Y. Li, L. Luo, and C. Q. Ma, "Solution-processed MoO_3:PEDOT:PSS hybrid hole transporting layer for inverted polymer solar cells," ACS Appl. Mater. Interfaces (submitted).
[22]W. W. Li, K. H. Hendriks, A. Furlan, W. S. C. Roelofs, M. M. Wienk, and R. A. J. Janssen, J. Am. Chem. Soc. **135**, 18942 (2013).
[23]P. Schilinsky, C. Waldauf, and C. J. Brabec, Appl. Phys. Lett. **81**, 3885 (2002).
[24]F. L. Zhang, A. Gadisa, O. Inganas, M. Svensson, and M. R. Andersson, Appl. Phys. Lett. **84**, 3906 (2004).
[25]Y. H. Zhou, F. L. Zhang, K. Tvingstedt, S. Barrau, F. H. Li, W. J. Tian, and O. Inganas, Appl. Phys. Lett. **92**, 233308 (2008).
[26]S. Barth, U. Wolf, H. Bassler, P. Muller, H. Riel, H. Vestweber, P. F. Seidler, and W. Riess, Phys. Rev. B **60**, 8791 (1999).
[27]W. C. Yang, Y. Yao, and C. Q. Wu, Org. Electron. **14**, 1992 (2013).
[28]S. B. Hacene and T. Benouaz, Phys. Status Solidi A **211**, 862 (2014).
[29]C. F. Zhang, S. W. Tong, C. Y. Jiang, E. T. Kang, D. S. H. Chan, and C. X. Zhu, IEEE Trans. Electron Devices **57**, 397 (2010).

Reuse of AIP Publishing content is subject to the terms at: https://publishing.aip.org/authors/rights-and-permissions. Download to IP: 141.215.185.157 On: Mon, 19 Sep 2016 13:23:39